Demosaicking Recognition with Applications in Digital Photo Authentication based on a Quadratic Pixel Correlation Model

Yizhen Huang *
Shanghai Video Capture Team
ATI Graphics Division, AMD Inc.
huang.yizhen@gmail.com

Yangjing Long
Department of Mathematics
Shanghai Jiaotong University
longyangjing@hotmail.com

Abstract

Most digital still color cameras use a single electronic sensor (CCD or CMOS) overlaid with a color filter array. At each pixel location only one color sample is taken, and the other colors must be interpolated using neighboring samples. This color plane interpolation is known as demosaicking, which is one of the important tasks in a digital camera pipeline. Demosaicked images possess spatially periodic inter-pixel correlation. In this paper, such correlation is expressed in a quadratic form, and Principal Component Analysis is applied to filter out intrinsic scene correlation. A decision mechanism using BP neural networks and a majority-voting scheme is designed to recognize demosaicking correlation and authenticate digital photos. Experiments show that, the proposed method can accurately classify images by demosaicking algorithms or source cameras, and it is effective to detect rendering forgeries. The sensitivity and robustness of the method are also verified. This algorithm-independent approach is especially useful when demosaicking algorithm is only available in form of binary code or integrated circuit without technical detail.

1. Introduction

Due to the limitation of hardware, most digital still color cameras use a single electronic sensor (CCD or CMOS) overlaid with a Color Filter Array (CFA), in a way that each sample point captures only one sample of the color spectrum.

The most frequently used CFA pattern is the Bayer CFA pattern [1], a schematic diagram of which is shown in Figure 1, where R, G, and B denote red, green and blue color filters, respectively. In this pattern, the red and blue pixels are sampled on rectilinear lattices, while the green pixels are sampled on a quincunx lattice. Typically, CFA pattern design is in accordance with the principle that the luminance channel (green) needs to be sampled at a higher rate than the chrominance channels (red and blue). The choice for green as 'representative' of the luminance is due to the fact that the luminance response curve of the eye peaks at around the frequency of green light (around 550 nm).

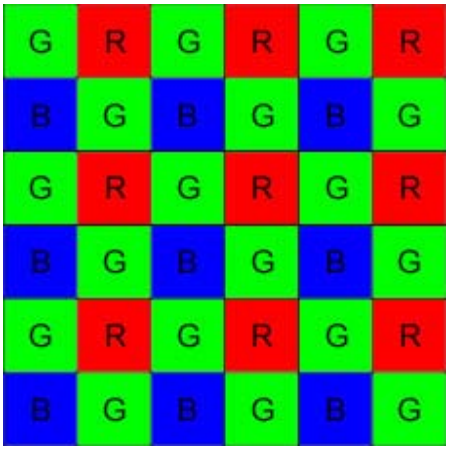

Figure 1. The Bayer CFA pattern

Since, at the location of each pixel, only one color sample is taken, the other colors must be interpolated from neighboring samples. This color plane interpolation is often referred to as demosaicking, which is one of the important tasks in a digital camera pipeline. If demosaicking is not performed appropriately, images suffer from highly-visible color artifacts. Therefore it is a key technology in most commercial camera systems. It has been extensively studied since the invention of the Bayer CFA pattern (see, for example, [2] and [3] for a survey).

Demosaicked images possess spatially periodic inter-pixel correlation. In this paper, such correlation is expressed in a quadratic form, and Principal Component Analysis is applied to filter out intrinsic scene correlation. A decision mechanism using BP neural networks and a majority-voting scheme is designed for demosaicking correlation recognition. This method is another new approach using camera hardware characteristics as clues for digital photo authentication.

Digital photo authentication is becoming increasing important. This is mainly due to the fact that, nowadays,

* This work was done when Yizhen Huang was studying at Department of Computer Science and Engineering, Shanghai Jiaotong University.

978-1-4244-2243-2/08/$25.00 ©2008 IEEE

photo-editing techniques have been very mature (see [4-6] for example). Beside its positive side such as reducing production cost, boosting and diversifying content etc., photo-editing also brings out series problems: do photographs reflect the real situation in the past? This has consequently invalidated the legal potency of photographs. There have been various works for digital photo authentication, e.g. [7] utilizes various kinds of pixel defects caused by hardware; [8] proposed 34 features which could be used by a classifier to identify the source camera of an image in a blind manner.

The rest of the manuscript is arranged as follows: Section 2 presents the proposed approach and its rationale analysis; Section 3 is the experimental results for categorizing both artificially demosaicked images and commercial digital cameras produced photos. Finally, Section 4 is the conclusion with some discussions.

2. The Proposed Method

2.1. Quadratic Pixel Correlation Model

Denote $I(\cdot)$ as one of the red, green, or blue channels. If pixel (x,y) is correlated to some other pixels linearly, it can be expressed as a weighted sum of these pixels:

$$I(x,y)=\sum_{i=1}^{N}\alpha_i I(x+\Delta x_i, y+\Delta y_i) \quad (1)$$

Where N is the number of correlated pixels, α_i, Δx_i and Δy_i are the weight, x offset and y offset of the ith correlated pixel respectively. The set consisting of offset coordinates $(\Delta x_i,\Delta y_i)$ for $1\le i\le N$ is referred to as correlated pixel set.

As a result of demosaicking, one color sample is correlated to their neighboring samples. Because the color filters in a CFA are typically arranged in periodic pattern, such correlation should demonstrate periodicity. Based on this, we assume that the correlated pixel set and its correspondent weights α_i of every pixel in $I(\cdot)$ is identical.

Certainly this hypothesis is unrealistic, because a channel independent linear model is overly simplistic when compared to the highly non-linear nature of most demosaicking algorithms. This means the left and right sides of Eq.(1) are usually unequal and may differ greatly. Regarding the right side of Eq.(1) as a filter F applied to $I(\cdot)$ (denoted as $F(I(\cdot))$), and accumulating the Mean Square Error of the two sides over $I(\cdot)$ gives:

$$MSE(F(I(\bullet)),I(\bullet))=\frac{1}{WH}\sum_{x=1}^{W}\sum_{y=1}^{H}\left|\sum_{i=1}^{N}\alpha_i I(x+\Delta x_i,y+\Delta y_i)-I(x,y)\right|^2 \quad (2)$$

Where W and H are the width and height of the image respectively.

By adding a virtual correlated pixel with $\alpha_{N+1}=-1$, $\Delta x_{N+1}=\Delta y_{N+1}=0$, Eq.(2) becomes a more orderly form:

$$MSE(F(I(\bullet)),I(\bullet))=\frac{1}{WH}\sum_{x=1}^{W}\sum_{y=1}^{H}\left|\sum_{i=1}^{N+1}\alpha_i I(x+\Delta x_i,y+\Delta y_i)\right|^2 \quad (3)$$

Expanding Eq.(3) gives a quadratic form with respect to $X=\{\alpha_1, \alpha_2, \ldots, \alpha_{N+1}\}^T$:

$$MSE(F(I(\bullet)),I(\bullet))=X^T AX \quad (4)$$

Where

$$A(i,j)=\frac{1}{WH}\sum_{x=1}^{W}\sum_{y=1}^{H}I(x+\Delta x_i,y+\Delta y_i)\times I(x+\Delta x_j,y+\Delta y_j),$$
$$(1\le i,j\le N+1)$$

Having noticed that, the coefficient matrix A contains complete information for determining the variable vector X, we do not try to obtain X. Instead, A is taken directly for further analysis.

		Δ		
	Δ	Δ	Δ	
Δ	Δ	⊗	Δ	Δ
	Δ	Δ	Δ	
		Δ		

Figure 2. Schematic of an empirically chosen correlated pixel set, where ⊗ denotes the pixel under consideration, and Δ denotes correlated pixels.

It is found empirically that, the correlated pixel set illustrated in Figure 2 gives good results. Thus N=12 and A is with dimension 13 by 13.

2.2. Principal Components Analysis

The numerical values of the elements of A are substantially large, and it is their variations and fluctuation that contains demosaicking characters and information. Thus the following operation is performed on A:

$$A^*(i,j)=[A(i,j)-\bar{A}]/\bar{A}, \quad (1\le i,j\le N+1) \quad (5)$$

Where $\bar{A}=\frac{1}{(N+1)^2}\sum_{1\le i,j\le N+1}A(i,j)$.

It is commonsense that, different images have different scenes and pixel intensity patterns. The actual inter-pixel correlation of an image is a combination of both scene correlation and demosaicking correlation. How to shake off the effects of the pre-existing correlation due to scene brightness away from the matrix A^* is the major difficulty for demosaicking recognition.

We discovered that, scene correlation generally distributes evenly over Principal Components Analysis (PCA) space of A^* while demosaicking correlation clusters at dimensions corresponding to large eigenvalues. Figure 3(a-b) compares the distribution spaces before and after the PCA transform.

Naturally, this leads to the idea of performing PCA on A^* and then analyzing its principal components:

Represent the matrix A^* as a N^2 dimensional vector β. Assume there are L images to form a training set $\{\beta_1, \beta_2\ldots,$

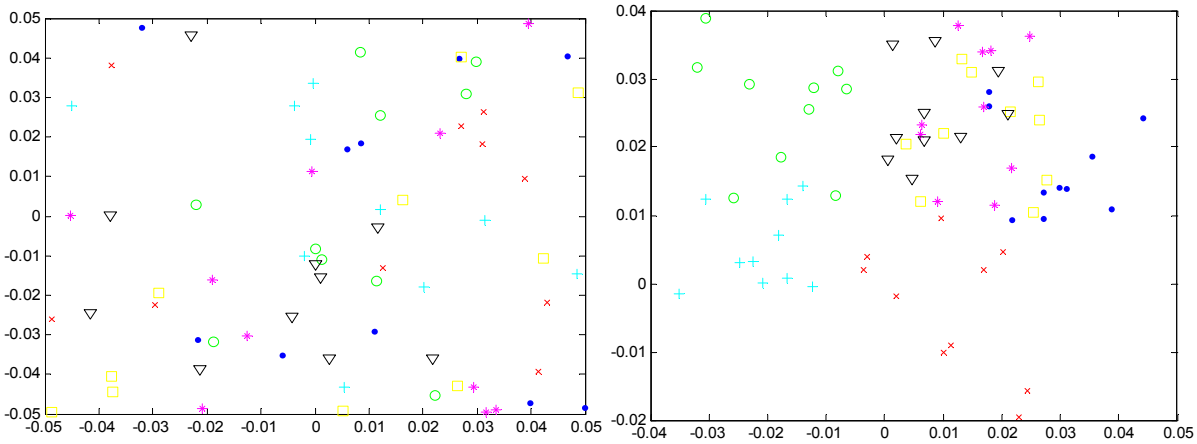

Figure 3. 2D distribution plot of the 6 demosaicking algorithms in the experiments in Subsection 3.1, whrere black triangles, green circles, red forks, yellow squares, viridescent crosses, pink stars, and blue dots stand for no-demosaick (original image), bilinear, bicubic, constant hue-based, median filter, gradient-based, and TBVNG algorithms respectively. For display purpose, only the results of 10 images are randomly chosen and drawn among the 100 for each algorithm. (a) is the space of $A(1,1)$ and $A(1,2)$. (b) is the space of the two most significant principal components Γ_1 and Γ_2. Even in this reduced 2D space, these demosaicking algorithms are, to some extend, clearly separable in (b).

$\beta_L\}$. The average vector is $\overline{\beta}=\frac{1}{L}\sum_{i=1}^{L}\beta_i$, and the difference vectors are $\beta_i^*=\beta_i-\overline{\beta}$, i=1,2,…L. So the estimate of the covariance matrix can be written as $C=[\beta_1^*, \beta_2^*\ldots, \beta_L^*][\beta_1^*, \beta_2^*\ldots, \beta_L^*]^T/(L-1)$.

Compute the eigenvalues and eigenvectors of C, denoted as $\{\lambda_1, \lambda_2\ldots, \lambda_L\}$ and $\{\xi_1, \xi_2\ldots, \xi_L\}$ ($\xi_1\geq\xi_2\ldots\geq\xi_{L-1}\geq\xi_L$) respectively. Choose M eigenvectors with the M largest eigenvalues to form the feature vector $V=[\lambda_1, \lambda_2\ldots, \lambda_M]^T$. Experiments show that M=15 is enough. Finally, β_i^* (i=1,2,…L) is turned into $\Gamma_i=V\beta_i^*$ with reduced dimension.

2.3. Neural-Network Design

We also tried SVM (Support Vector Machine) as the classifier, however, the experimental results are far from that of neural networks, in respect of the fact that, the highly non-linear nature of demosaicking interpolation compels the SVM to quite high dimension for the sake of depicting such correlation.

Basically 3-layer feed-forward BP neural networks are adopted as shown in Figure 4: The input layer has M=15 neurons, the hidden layer has 50 neurons and the output layer has 1 neuron indicating the degree of difference between training vectors previously fed to the network and the current input vector. The sigmoid transfer function of the hidden layer is $tansig(x)=2/(1+exp(-2x))-1$ and that of the output layer is $logsig(x)=1/(1+exp(-x))$. The training algorithm is selected to be the Scaled Conjugate Gradient method [13].

The training set is $\{\Gamma_1, \Gamma_2\ldots, \Gamma_L\}$, and the target value is 0. L should be elaborately selected. According to experience from experiments, L=100 balances the contradiction between the computing cost for training and the network performance satisfactorily.

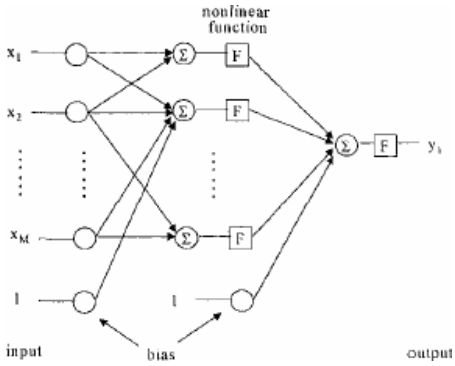

Figure 4. Schematic of a 3-layer BP neural network

Interestingly, the technical means used here is quite similar to face recognition with PCA and neural-networks, if regarding A^* in Eq.(5) as a grayscale face image.

2.4. Making Decisions

Denote D as the set of all demosaicking algorithms. $D^*=D\cup\{\varnothing\}$, where $\varnothing$ denotes doing nothing, leaving the original $I(\cdot)$ intact. Demosaicking recognition is actually to find a $d\in D^*$, which has the highest probability that has been performed on $I(\cdot)$. Or from the perspective of our training and simulating mechanism, demosaicking recognition is to attribute $I(\cdot)$ to one of the $|D^*|$ classes of

training images that is the closest to $I(\cdot)$ measured in the demosaicking characteristics space.

Different classes of training images hereby should be fed to different networks. The following 2 points are taken for considering the number of networks to keep:

(1) It is natural to store different networks for $d_1, d_2 \in D^*$, $d_1 \neq d_2$.

(2) As seen in [2-3,9-12], in the same demosaicking algorithm, demosaicking operators performed on the luminance channel (green) and the chrominance ones (red and blue) differ greatly. Therefore it is necessary to store different networks for them. For better results, our experiments keep 3 networks, one for each channel.

Thus we store weights and bias values of $|D^*|=|D|+1$ networks for each channel, and $3(|D|+1)$ totally. For expression convenience, these networks are represented as a 2-D array, in which $network[d][c]$ stands for the network with training images demosaicked by algorithm $d \in D^*$ on color channel c. And $network[d][c](I(\cdot))$ is the output value of this network when simulating $I(\cdot)$.

For a given $I(\cdot)$ on color channel c, the larger the $|network[d][c](I(\cdot))|$ is, the less likely $I(\cdot)$ is demosaicked by d. And the final decision d satisfies that, for any other $d' \neq d$, $d' \in D^*$, $|network[d][c](I(\cdot))| < |network[d'][c](I(\cdot))|$.

2.5. Combine Three Channels Together

It is seen that our method in the previous 4 subsections is channel-independent i.e. a "relatively" independent classification judgment is made for each channel. However, it is inadequate to say "absolute" independence because cross-correlation between channels exists (see, for example, Section II-A of [14] where the degree of inter-channel correlation is quantified).

Hence, it is feasible to employ the majority-voting scheme [15] to enhance the reliability of the classifier: An image is recognized as demosaicked by an algorithm, only if a consensus is reached among the 3 channels i.e. at least 2 channels make the same judgment; otherwise a rejection is given.

This scheme may be enhanced by assigning different weights to different channels according to their inter-channel correlation.

3. Experiments

To evaluate the proposed technique, it is applied on both artificially demosaicked images and digital photos. In both experiments, each network is trained by 100 images and simulated by other 100 images. Figure 5 displays some example images from our image database.

For ease of notation, an indicator κ is defined for a given $I(\cdot)$ on color channel c demosaicked by algorithm d_c:

$$\kappa = \min\{|network[d][c](I(\bullet))| \mid d \in D^* - \{d_c\}\} - |network[d_c][c](I(\bullet))| \quad (6)$$

$\kappa > 0$ means $network[d_c][c]$ is less than all other $network[d][c]$ for $d \neq d_c$, and a correct classification decision is made by our method; otherwise, our method fails on this channel. Only if our method fails on at least 2 channels of an image, a misjudgment or a rejection is given by the major-voting scheme. The larger the κ is, the higher the confidence is.

Figure 5. Some example images from our image database

3.1. Artificially Demosaicked Images

The bilinear, bicubic [2-3], constant hue-based [9], median filter [10], gradient-based [11], and TBVNG (Threshold-Based Variable Number of Gradients) [12] demosaicking algorithms are performed to demosaick the original images and results in 7 sets of images including the original image set. The results are shown in Figure 6(a). Because the bilinear and constant-hue based interpolation use exact the same algorithm on the green channel which are theoretically impossible to differentiate, their corresponding κ values are very close to 0. Nevertheless, this does not harm the final recognition results too much, since the majority voting scheme can neglect failure on a single channel.

3.2. Photos Produced by Commercial Cameras

We also test the efficacy of the proposed method on photos produced by 4 commercially available digital cameras: DEC U350, SONY P73, Kodak Z730 and Olympus IS5000. All cameras are set to store photos in uncompressed format. Besides, we add a class of cartoon images for comparison. Figure 6(b) lists the results, where the recognition rates and the confidence κ of our method on real cameras is obviously lower, compared to that on ideal demosaicking operators in Subsection 3.1. This is natural considering the fact that, noise induced in different stages of the image formation pipeline of a digital camera more or less corrupts the periodic inter-pixel correlation left by demosaicking.

3.3. Sensitivity and Robustness

It is important to quantify the sensitivity and robustness of a technique for practical use. Therefore the trained networks in Subsection 3.2 are simulated using images with typical distortions: (1) JPEG compression (2) additive white Gaussian noise (3) gamma correction (4) median filter smoothing.

The results are displayed in Figure 7(a-d): Our method is to some extend endurable to JPEG compression; and its recognition rates decline gracefully with decreasing SNR of Gaussian noise and increasing $|\gamma-1|$ in gamma correction. Such decline on performance is expected, since noises distort inter-pixel correlations. Notably, our method is so sensitive to median filters that a 7x7 median filter can completely invalidate it. This is due to the fact that, a pixel value is very likely to be moved to its neighborhood during median filtering and thus pixel neighborhood correlation is utterly destroyed.

3.4. Digital Photo Authentication

The last of the experiments is to apply our technique to digital photo authentication. Figure 8(d-f) are images containing perceptually plausible forgeries created using Adobe Photoshop, with their suspicious regions cropped. For comparison purpose, their corresponding real photos taken by a DEC U350 camera are displayed as Figure 8(a-c). The real photos, the tampered photos, and the cropped counterfeit regions are tested by our method with the neural networks of DEC U350 in Subsection 3.2. The results are listed in Table 1.

	Fig. 8(a,d)	Fig. 8(b,e)	Fig. 8(c,f)
Original image	0.512	0.189	0.621
Tampered image	1.052	0.471	0.869
Cropped region	1.327	2.539	1.921

Table 1. The absolute values of the output of the networks DEC U350 (averaged on the 3 channels)

	Fig. 9(a,d)	Fig. 9(b,e)	Fig. 9(c,f)
Original image	0.691	0.215	0.543
Tampered image	0.924	0.512	0.982
Cropped region	1.510	2.346	1.832

Table 2. The absolute values of the output of the networks SONY P73 (averaged on the 3 channels)

	Fig. 10(a,d)	Fig. 10(b,e)	Fig. 10(c,f)
Original image	0.746	0.313	0.509
Tampered image	0.989	0.624	0.941
Cropped region	1.537	1.883	2.036

Table 3. The absolute values of the output of the networks Kodak Z730 (averaged on the 3 channels)

	Fig. 11(a,d)	Fig. 11(b,e)	Fig. 11(c,f)
Original image	0.385	0.435	0.473
Tampered image	2.716	1.373	1.257
Cropped region	1.742	1.932	2.039

Table 4. The absolute values of the output of the networks Olympus IS5000 (averaged on the 3 channels)

For clarity, Figure 9(a-f), Figure 10(a-f) and Figure 11(a-f) are organized in the format very similar to Figure 8(a-f), and their real photos are taken by SONY P73, Kodak Z730 and Olympus IS5000 cameras respectively. And analogously, they are tested by the neural networks of SONY P73, Kodak Z730 and Olympus IS5000, trained in Subsection 3.2. The results are listed in Table 2-4.

In Table 1-4, the network output indicates the difference between the tested images and the images used for training, and it is seen that, detection on a smaller suspicious region provides more evident clues to reveal forgeries rather than detection on the entire image. Besides, it is natural to think that the region to be detected should be large enough to statistically demonstrate inter-pixel demosaicking correlation periodicity.

Having noticed this, we try to improve this method by refining the selected rectangular window for test to be a manually selected pixel set, i.e. a more precise shape enclosing the suspicious region rather than a rectangle. And this selected pixel set is then utilized for the sum operation in Eq.(4). But the improvement on the discernability from the network output between the original and the tampered images is almost negligible. Due to the limited space, the corresponding results are not listed. It is apprehensible, because the matrix A^* is the outcome of statistical correlation, instead of the correlation of a few individual pixels.

While effectively tackling the aforementioned rendering forgeries, our method is powerless to detect copy-move forgeries. With the Lazy Snapping tool [6], Figure 12(d) is synthesized from Figure 12(a,b), which are both taken by a DEC U350 camera. No matter how to select the tested window in Figure 12(d) (within either foreground or background, or across their border), the network output shows no abrupt change. However, if the photos synthesized are taken by different cameras, for example, Figure 12(e) is synthesized from Figure 12(a,c) taken by a DEC U350 camera and a SONY P73 camera respectively. The network output of DEC U350 within foreground and background are 0.2-0.8 and 0.7-1.1 and that of SONY P73 are 0.8-1.5 and 0.1-1.0 respectively, which is still differentiable to some degree.

4. Conclusion

Photos produced by most digital still color cameras are demosaicked. Because the color filters in a CFA are typically arranged in a periodic pattern, demosaicked images should demonstrate spatially periodic inter-pixel correlation. In this paper, we present a quadratic pixel correlation model, in which such correlation is expressed in a quadratic form. Based on this model, Principal Component Analysis is applied to filter out intrinsic scene correlation. A decision mechanism using BP neural networks and a majority-voting scheme is designed for demosaicking correlation recognition and digital photo authentication. Experimental results verify the validity and practicability of this method. If taking inter-channel

correlation ([14] provides some statistics) into consideration rather than using the majority-voting scheme to combine the 3 channels together, better results may be achieved.

Our method is a general-purpose approach for demosaicking recognition, which does not depend on technical details of the demosaicking algorithms. So it is especially useful when the demosaicking algorithms to be detected are very complicated, or only available to be used without its technical detail released due to specific commercial or political reasons.

References

[1] B. E. Bayer, Color imaging array, U.S. Patent, No. 3,971,065, 1976.

[2] B. K. Gunturk, J. Glotzbach, Y. Altunbasak, R. W. Schafer, and R. M. Mersereau, Demosaicking: Color filter array interpolation in single chip digital cameras, IEEE Signal Processing Magazine, 22(1):44-54, 2005.

[3] R. Ramanath, W. E. Snyder, G. L. Bilbro and W. A. Sander III, Demosaicking methods for Bayer color arrays, Journal of Electronic Imaging, 11(3):306-315, 2002.

[4] Y. Boykov and M. P. Jolly, Interactive graph cuts for optimal boundary & region segmentation of objects in N-d images, Proceedings of ICCV 2001, pp.I: 105-112.

[5] Y. Y. Chuang, B. Curless, D. H. Salesin and R. Szeliski, A Bayesian approach to digital matting, Proceedings of CVPR 2001, pp.II: 264-271.

[6] Y. Li, J. Sun, C. K. Tang and H. Y. Shum, Lazy Snapping, Proceedings of ACM Siggraph 2004, pp. 303-308.

[7] J. Geradts, J. Bijhold, M. Kieft, K. Kurosawa, K. Kuroki and N. Saitoh, Methods for identification of images acquired with digital cameras, SPIE Vol. 4232, pp. 505-512, 2001.

[8] M. Kharrazi, H. T. Sencar and N. Memon, Blind source camera identification, Proceedings of ICIP 2004, pp.709-712.

[9] D. R. Cok, Signal processing method and apparatus for producing interpolated chrominance values in a sampled color image signal, U.S. Patent, No. 4,642,678, 1986.

[10] W. T. Freeman, Median filter for reconstructing missing color samples, U.S. Patent, No. 4,724,395, 1988.

[11] C. A. Laroche and M. A. Prescott, Apparatus and method for adaptively interpolating a full color image utilizing chrominance gradients, U.S. Patent, No. 5,373,322, 1994.

[12] E. Chang, S. Cheung and D. Y. Pan, Color filter array recovery using a threshold-based variable number of gradients, SPIE vol. 3650, pp. 36-43, 1999.

[13] A.F. Moller, A scaled conjugate gradient algorithm for fast supervised learning, Neural Networks, 6(4):525-533, 1993.

[14] B. K. Gunturk, Y. Altunbasak and R. M. Mersereau, Color plane interpolation using alternating projections, IEEE Transactions on Image Processing, 11(9):997-1013, 2002.

[15] L. Lam and C.Y. Suen, Application of majority voting to pattern recognition: An analysis of its behavior and performance, IEEE Transactions on Systems, Man and Cybernetics, 27(5):553–568, 1997.

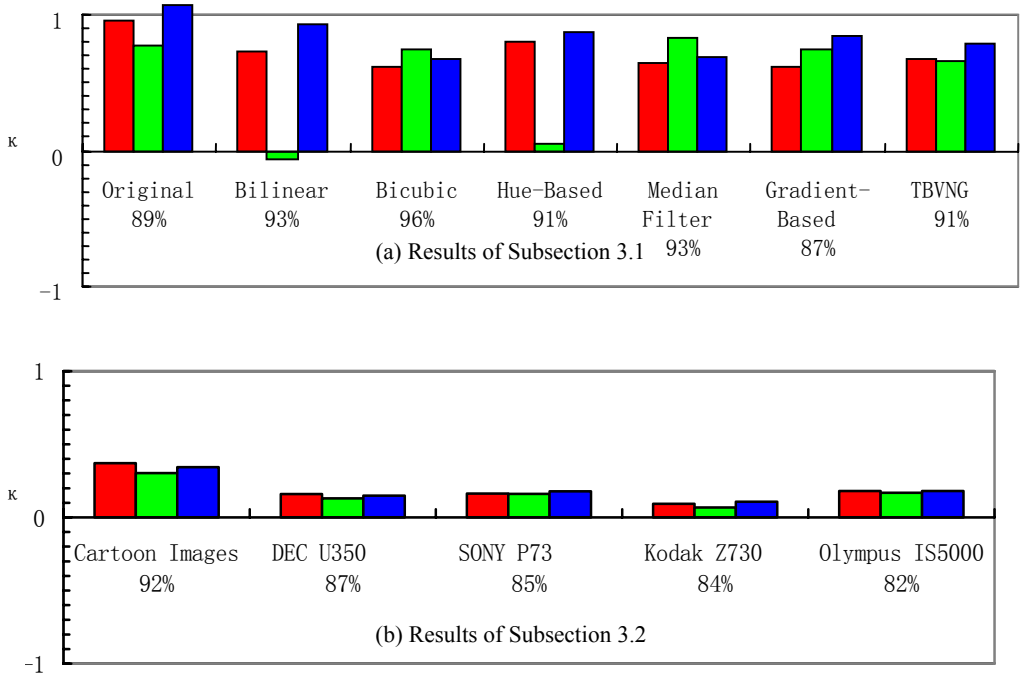

Figure 6. (a-b) Experimental results of Subsections 3.1 and 3.2, where each grid on the horizontal axis displays 3 colored strips for the results of the red, green, blue channels of a demosaicking algorithm/camera, the vertical axis is the average κ over 100 images. Recognition rate is labeled under the name of each demosaicking algorithm/camera.

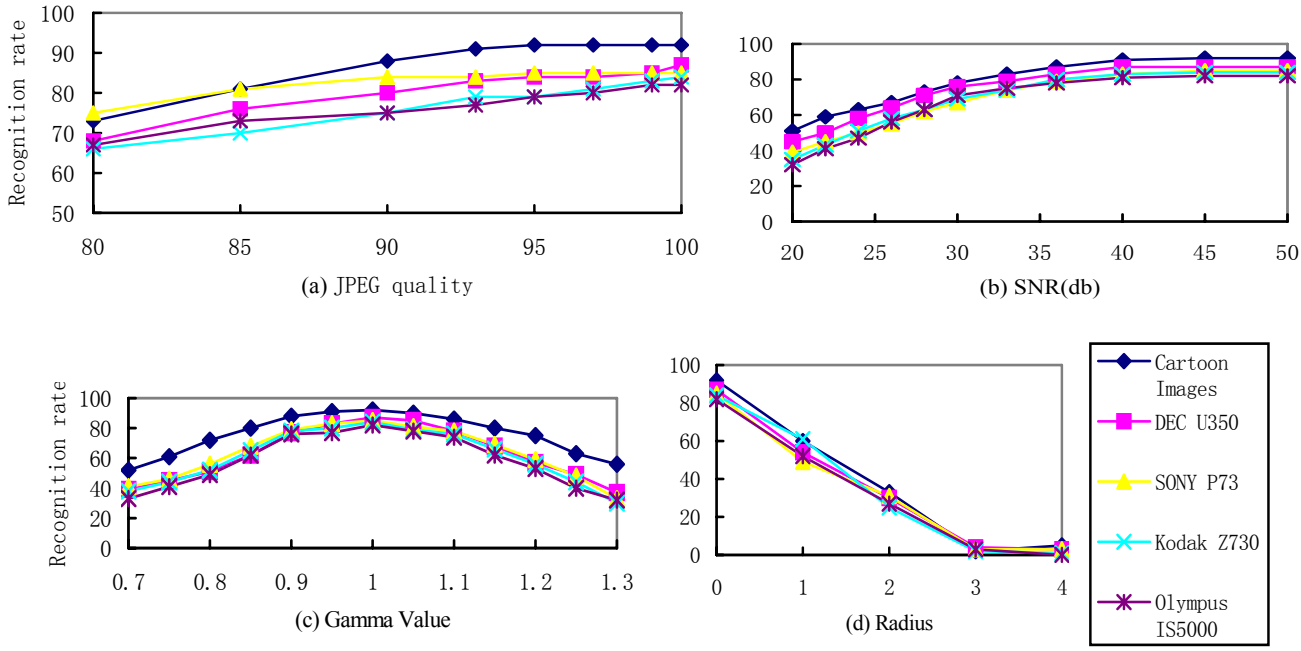

Figure 7. (a-d) Recognition rates for different cameras as a function of JPEG quality, SNR (Signal-to-Noise Ratio) of white Gaussian noise, the γ value of gamma correction, radius of median filter respectively. Each data point corresponds to a recognition rate over 100 images.

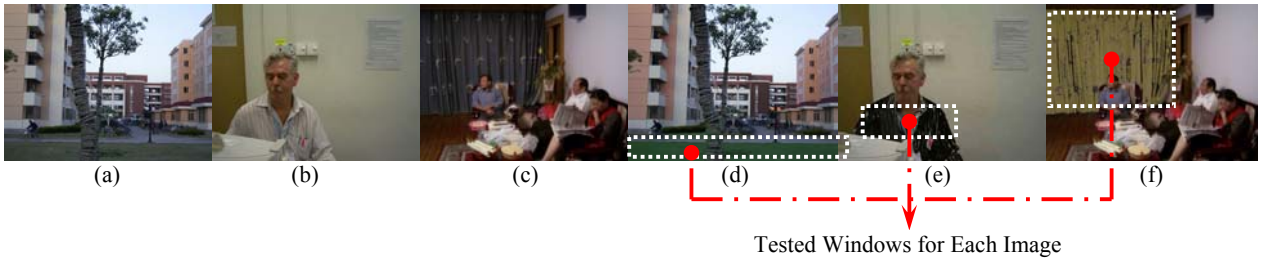

Figure 8. (a-c) 3 real images taken by a DEC U350 camera. (d) It is tampered from (a) in the following places: The kind of bald lawn becomes grass green; the lower part of the rope binding the tree in the middle portion of the photo is adhered to lichen; the street lamp is "lighted"; and the old pink wall of the two apartment buildings at both left and right parts of the photo is "repainted". (e) The man is clothed with a black sweater, outside his stripped T-shirt originally in (b). (f) The curtain at the rear of the room in (c) is colored with brown yellow. The tested windows are suspicious and cropped for detection.

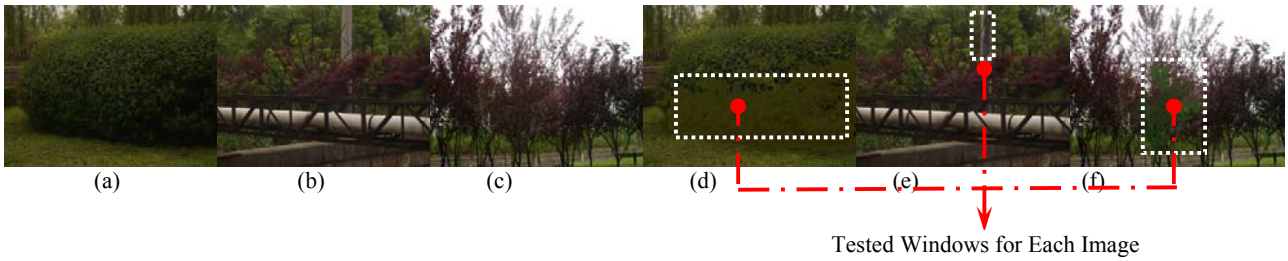

Figure 9. (a-c) 3 real images taken by a SONY P73 camera. (d) It is tampered from (a) with the green leaves of the tree faded with yellow. (e) The electric pole cropped is scorched. (f) The red leaves of one of the maples is turned into green color.

Figure 10. (a-c) 3 real images taken by a Kodak Z730 camera. (d) It is tampered from (a) with the bright sky darken. (e) The stone is attached with some lichen at its dimmest portion, it is not very noticeable though. (f) The pink exterior wall of the building is painted with a little bit deeper color.

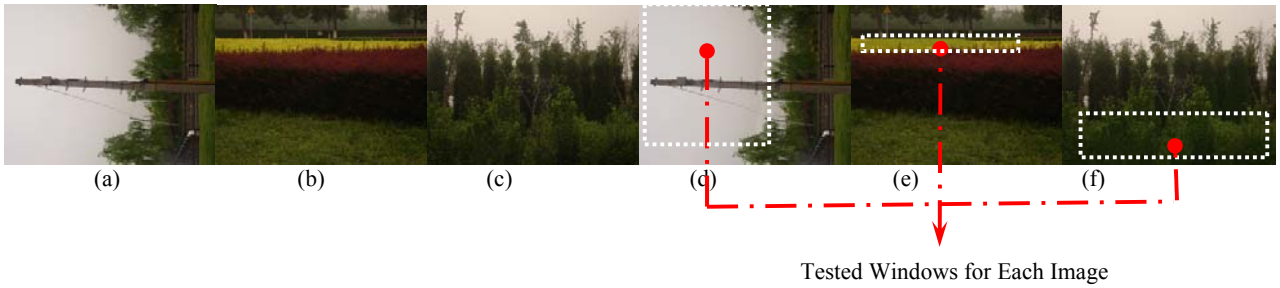

Figure 11. (a-c) 3 real images taken by a Olympus IS5000 camera. (d) It is tampered from (a) with the sky darken. (e) The yellow flowers at the farthest becomes a little greenish. (f) The bottom part of the green grove is covered with emerald mist.

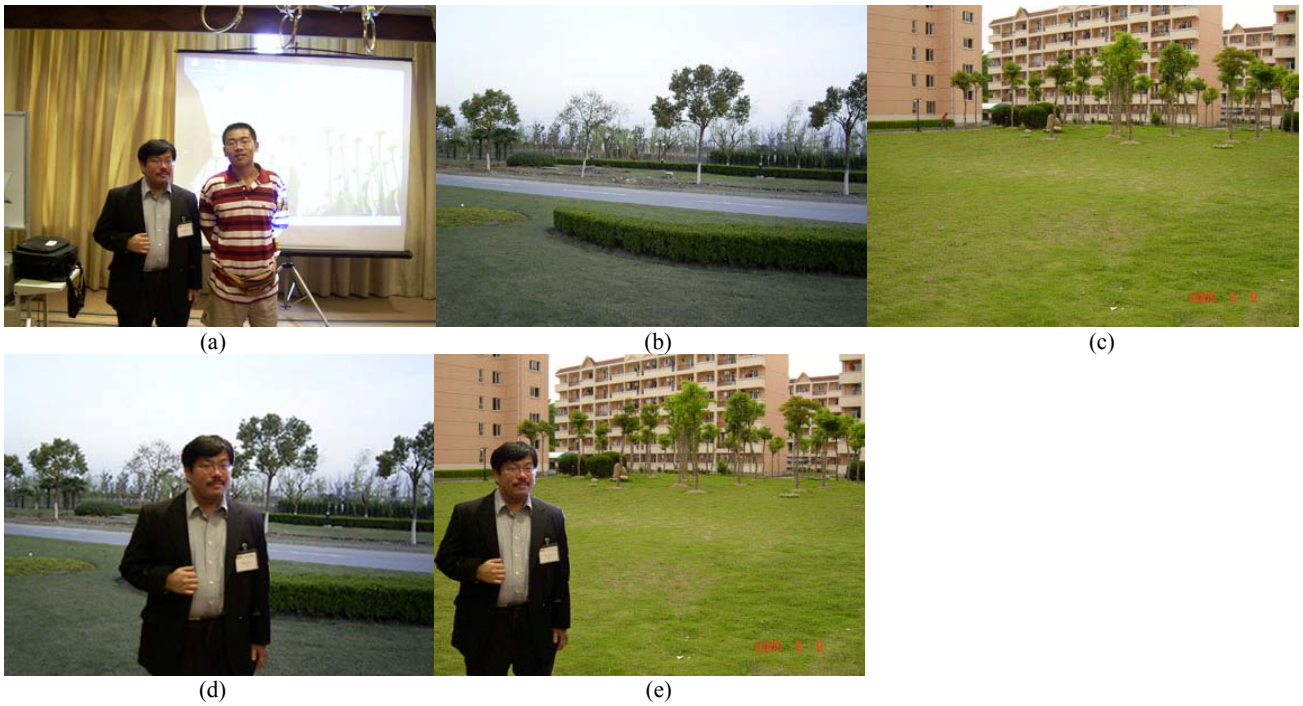

Figure 12. (a-b) 2 real images taken by a DEC U350 camera. (c) A real images taken by a SONY P73 camera. (d) The shorter person in (a) is extracted and synthesized with new background scene (b). (d) The person in (a) is synthesized with another background (c).